ELSEVIER

Enhanced heat transfer in round tubes with porous inserts

Mehmet Sözen
Department of Mechanical Engineering, Southern University, Baton Rouge, LA, USA

T. M. Kuzay
Experimental Facilities Division, Advanced Photon Source, Argonne National Laboratory, Argonne, IL, USA

The modeling and numerical simulation studies of fluid flow and enhanced heat transfer in round tubes filled with rolled copper mesh are described in this paper. The tubes were subjected to uniform heat flux, and water was used as the energy transport fluid. The numerical solution was obtained by a finite difference code developed in this investigation. The fluid flow was modeled by a modified Ergun–Forchheimer–Brinkman equation. The energy transfer was based on a single equation model; i.e., local thermal equilibrium between the solid and fluid phases. Variations of the local Nusselt number and local heat transfer coefficient were obtained accurately by the use of nonuniform grid size in the radial direction in the numerical simulations. The numerical results obtained were compared with the experimental results obtained by the Experimental Facilities Division at Argonne National Laboratory, and the two were in good agreement.

Keywords: porous media; fibrous; heat transfer

Introduction

In high-heat-flux applications, it is desirable to enhance the heat transfer in the cooling channels used for cooling critical components. Among these applications, cooling of the front-end and beamline components of synchrotrons is an important part. Kuzay (1990), in an extensive study regarding Biot number dependency of heat transfer enhancement techniques, has shown that, with a good choice of the material (such as oxygen-free, high-conductivity (OFHC) copper), heat transfer in the cooling components will be convection limited. Therefore, efforts in heat transfer enhancement should concentrate on improving the heat transfer in the cooling channels; i.e., on the convective heat transfer side. To this end, cooling channels with porous inserts have been an attractive choice, because the effective thermal conductivity of such a porous medium could be an order of magnitude higher than that of water. Use of such channels, therefore, could increase the local heat transfer coefficients dramatically. This principle has been widely used in the Advanced Photon Source front-end and beamline component designs at Argonne National Laboratory (ANL) (Kuzay 1994). Slightly different arrangements, under the name of "pumped single-phase porous media heat exchangers," have been developed for other potential applications, such as cooling of high-power optical structures and cooling of susceptors for plasma processing. One such unit, which was tested at Sandia National Laboratories, was reported to have handled a heat flux of 5.6 MW/m^2 (Rosenfeld and Lindemuth 1993).

To understand the heat transfer phenomena in cooling channels with copper mesh inserts, an experimental program was initiated at the Experimental Facilities Division at ANL. Copper tubes internally brazed to rolled copper meshes of known porosity were instrumented and carefully tested to obtain the heat transfer coefficient and the friction factor experimentally under uniform heat flux conditions (Kuzay et al. 1991). It has been observed that large heat transfer enhancement is possible using these porous conductive inserts in the cooling channels. Experimentally, relative to plain channels, up to a tenfold increase in the heat transfer coefficient has been obtained with the brazed porous inserts at the expense of highly increased pressure drop.

Experimental investigations dealing with both single- multiphase flows with phase change in tubes with porous inserts have been reported (Megerlin et al. 1974; Gortyshov et al. 1991). Although there is lack of investigations reported on modeling of this specific type of porous medium formed by rolled copper mesh, models developed for other types of porous media such as packed beds may be a good starting point (see, for example, Vafai and Sözen 1990; Poulikakos and Renken 1987).

In the present study, we develop a simple yet rigorous mathematical model and numerical code for simulating the heat transfer and fluid flow in the copper tubes with rolled copper mesh inserts brazed to the tube walls. The objective is to understand better the heat transfer and fluid flow phenomena in porous cooling channels. Moreover, once validated by the experimental results, the numerical code developed can be used for parametric studies.

Address reprint requests to Prof. M. Sözen, Department of Mechanical Engineering, Southern University, Baton Rouge, LA 70813, USA.

Received 28 June 1995; accepted 23 October 1995

Int. J. Heat and Fluid Flow 17: 124–129, 1996

655 Avenue of the Americas, New York, NY 10010

0142-727X/96/$15.00
SSDI 0142-727X(95)00095-X

In this investigation, an accurate model for the fluid flow is established based on the experimental data. Namely, the Ergun–Forchheimer equation is modified to represent the effect of the structure of the porous matrix under investigation on the fluid flow/pressure drop relationship. There is an unheated portion of approximately 2.5 diameters length on each end of the tube used in the experiments. Therefore, the flow is assumed to be hydrodynamically fully developed in the heated region. The common assumption of linear pressure variation along the tube is used in this study. Energy transfer is modeled based on local thermal equilibrium between the copper matrix and the water; i.e., a single-equation model.

Formulation and analysis

Modification of the Ergun–Forchheimer equation for porous matrix formed with rolled copper mesh

For fluid flow in a packed bed of spherical particles, the viscous and inertia effects are related to the pressure gradient by the Ergun equation (Ergun 1952)

$$-\frac{dP}{dx} = 150\frac{\mu u_m}{D_p^2}\frac{(1-\epsilon)^2}{\epsilon^3} + 1.75\frac{\rho u_m^2}{D_p}\frac{(1-\epsilon)}{\epsilon^3} \tag{1}$$

Because of the nature of the tortuous paths in the rolled copper mesh that forms the porous matrix under study, the momentum equation expressed in a form similar to the Ergun equation will be modified; i.e., the two constants in Equation 1 will be different to express different viscous and inertia effects in the porous matrix as compared to those in a packed bed. This is done as suggested by Cai (1993) by writing the modified equation as follows:

$$-\frac{dP}{dx} = C_L\frac{\mu u_m}{d_f^2}\frac{(1-\epsilon)^2}{\epsilon^2} + C_T\frac{\rho u_m^2}{d_f}\frac{(1-\epsilon)}{\epsilon^3} \tag{2}$$

where d_f represents a characteristic length, which is the fiber diameter of the copper mesh, and C_L and C_T are two empirical constants that are used to model the viscous and inertia effects accurately.

In the present study, the porous medium considered was rolled copper mesh inserted in round tubes. The porous matrix used in the first tube had 75% porosity and consisted of rolled copper mesh of size 203.2 × 203.2 × 0.32 mm; whereas, that used in the second tube had 85% porosity with a mesh size of 203.2 × 203.2 × 0.2032 mm. The tube inner diameter was 9.525 mm, and the heated tube length was 21.6 cm. The experimental data available for pressure gradient for different flow rates for each tube configuration provided the basis for the necessary analysis. C_L and C_T were determined from the experimental data by linear regression with the least-squares method. These values are listed in Table 1. Comparisons of these values with those of Ergun's (1952) equation reveal that, although the viscous effects are comparable to those of packed beds, the inertia effects are quite different, because the characteristics of the form drag are different due to different structure.

Table 1 Values of C_L and C_T

	C_L	C_T
Tube #1	177.181155	0.402619
Tube #2	156.172914	0.493956

Modeling of the constant wall-heat-flux problem

The model developed for analyzing the fluid flow and heat transfer in the porous round tube is based on the momentum equation developed in the previous section modified by the Brinkman (1947) extension as

$$-\frac{dP}{dx} = C_L\frac{\mu u}{d_f^2}\frac{(1-\epsilon)^2}{\epsilon^3} + C_T\frac{\rho u^2}{d_f}\frac{(1-\epsilon)}{\epsilon^3} - \frac{\mu}{\epsilon}\frac{1}{r}\frac{d}{dr}\left(r\frac{du}{dr}\right) \tag{3}$$

where u denotes the superficial velocity, and the last term on the right-hand side is the Brinkman term, which ensures the no-slip boundary condition at the wall.

Energy transfer is based on a one-equation model; i.e., local thermal equilibrium between the solid and fluid phases in the porous matrix. The transient energy equation is given for the axisymmetric problem as

$$\left(\epsilon\rho_f c_{p_f} + (1-\epsilon)\rho_s c_s\right)\frac{\partial T}{\partial t} + \rho_f c_{p_f} u\frac{\partial T}{\partial x} = \frac{\partial}{\partial x}\left(k_{\text{eff}_x}\frac{\partial T}{\partial x}\right) + \frac{1}{r}\frac{\partial}{\partial r}\left(k_{\text{eff}_r}\frac{\partial T}{\partial r}\right) \tag{4}$$

Notation

C_L	empirical constant in Equations 2 and 3
c_p	specific heat, J/kgK
C_T	empirical constant in Equations 2 and 3
d_f	fiber diameter, m
D	inner diameter of tube, m
D_o	outer diameter of tube, m
D_p	particle diameter, m
f	friction factor
h	heat transfer coefficient, W/m^{2}K
k	thermal conductivity, W/mK
$\dot{m}$	mass flow rate, kg/s
n	constant in Equation 5
Nu	Nusselt number
P	pressure, Pa
q''_w	inner wall heat flux, W/m^{2}K
r	coordinate variable in radial direction, m
R	inner radius of tube, m
Re	Reynolds number, $\rho u_m D/\mu$
t	time, s
T	temperature,°C
u	superficial velocity, m/s
x	coordinate variable in axial direction, m

Greek

α	multiplication factor in equation (7)
Δr	grid size in r-direction, m
ϵ	porosity
μ	dynamic viscosity, kg/m s
ρ	density, kg/m^3

Subscripts

eff	effective
f	fluid phase
m	mean (bulk)
o	outer wall
s	solid phase
w	inner wall

The effective thermal conductivity of the porous medium is based on the work of Koh and Fortini (1971) and modified by Januszewski et al. (1977) for felt metals. It is given as follows:

$$k_{\text{eff}_i} = k_s\left(\frac{1-\epsilon}{1+n\epsilon^2}\right) \tag{5}$$

where n is a constant taken to be equal to 10 in this study, and i represents either x or r. The first term in Equation 4 goes to zero at steady state. However, the solution procedure was based on an explicit finite difference numerical scheme, and, therefore, the transient term was maintained in the energy equation. The boundary conditions for the problem were

No-slip boundary condition:

at $r = R \quad u = 0$

Symmetry condition

$$\text{at} \quad r = 0 \qquad \frac{du}{dr} = 0 \tag{6}$$

The boundary conditions for the energy equation are

Inlet condition:

at $x = 0 \quad T = T_{\text{in}}$

Inner wall heat flux condition:

$$\text{at} \quad r = R \qquad q''_w = k_{\text{eff}} \left.\frac{\partial T}{\partial r}\right|_{r=R}$$

Symmetry condition;

$$\text{at} \quad r = 0 \qquad \left.\frac{\partial T}{\partial r}\right|_{r=0} = 0 \tag{7}$$

Numerical solution

Finite difference methods were used to obtain the solutions for the momentum and energy equations. To capture the variation of fluid velocity and the local heat transfer coefficient along the tube accurately, a very fine grid in the radial direction was necessary in the vicinity of the tube walls. To avoid costly CPU time, a variable grid was used in the radial direction. This was based on the *compound interest grid* in which each grid size is a constant multiple of the neighboring one. Mathematically, $\Delta r_{i-1} = \alpha(\Delta r_i)$, where α is the multiplication factor. With this arrangement, a very fine grid was obtained in the vicinity of the wall of the tube, while the grid size became coarser in the core region where the variations in both velocity and temperature occur less drastically.

The momentum and energy equations were solved independently because of the incompressible flow assumption. The nonlinear (Forchheimer) term in the momentum equation was linearized by Newton's method (Nakamura 1986). Second-order accurate finite difference approximations of the first and second derivatives were obtained by the Taylor expansion method. The resulting system of equations yielded a tridiagonal system of linear algebraic equations, the solution of which was obtained by the well-known Thomas algorithm (Anderson et al. 1984). A convergence criterion, which required less than a difference of 10^{-12} m/s between the values of the velocity at every nodal point in two consecutive iterations, was implemented.

The finite difference form of the energy equation was obtained by using Euler forward differencing for the temporal derivative term and second-order accurate central differencing for the spatial derivative terms. One exception to this was the treatment of the convective term in the energy equation ($u\partial T/\partial x$) for which *upwind differencing* was used rather than central differencing in order to make the numerical scheme stable. Because of the strong parabolic nature of the energy equation, at the nodes on the exit plane of the tube, the second derivative term in the x-direction was approximated by a second-order accurate backward differencing. The resulting finite difference equations yielded the temperature in explicit form, and, therefore, the temperature distribution was obtained by choosing an appropriate time-step that would make the numerical scheme stable. Because we were interested in the steady-state solution of the problem, we chose by trial and error a time-step close to the largest one that would yield a stable solution. Hence, the accuracy of the transient solution was not reliable, but that of the steady-state solution was. A value of 1.05 for the multiplication factor α and an optimum 51×51 mesh were found to yield satisfactory results with less than 0.6% difference in any computed temperature value when the mesh size was increased to 71×51 or 51×81.

Friction factor

The definition used in the experimental work was implemented into the numerical code as follows:

$$f = \frac{-\dfrac{dP}{dx}D}{\rho u_m^2/2} \tag{8}$$

where the mean velocity was computed numerically from

$$u_m = \frac{\displaystyle\int_0^R ur\,dr}{\displaystyle\int_0^R r\,dr} \cong \frac{\sum_i u_i r_{i+1/2}\left(\dfrac{\Delta r_i + \Delta r_{i-1}}{2}\right)}{\sum_i r_{i+1/2}\left(\dfrac{\Delta r_i + \Delta r_{i-1}}{2}\right)} \tag{9}$$

Because of symmetry, for $i = 1$, $\Delta r_i = \Delta r_{i-1}$, and so $(\Delta r_i + \Delta r_{i-1})/2 = \Delta r_1$.

Local heat transfer coefficient and the local Nusselt number

The local heat transfer coefficient was defined and calculated from the following:

$$h(x) = \frac{q''_w}{T_w(x) - T_m(x)} \tag{10}$$

and the local Nusselt number was defined as

$$\text{Nu}(x) = \frac{h(x)D}{k_f} = \frac{q''_w}{T_w(x) - T_m(x)}\frac{D}{k_f} \tag{11}$$

where w represents inner wall and m represents for mean (bulk). As in the case of the Nusselt number and the heat transfer coefficient, the bulk temperature was defined based on the properties of the fluid phase as follows:

$$T_m(x) = \frac{\displaystyle\int_0^R urT(x)\,dr}{\displaystyle\int_0^R ur\,dr} \cong \frac{\sum_i u_i r_{i+1/2} T_i(x)\left(\dfrac{\Delta r_i + \Delta r_{i-1}}{2}\right)}{\sum_i u_i r_{i+1/2}\left(\dfrac{\Delta r_i + \Delta r_{i-1}}{2}\right)} \tag{12}$$

Again, because of symmetry, for $i = 1$, $\Delta r_i = \Delta r_{i-1}$, and so $(\Delta r_i + \Delta r_{i-1})/2 = \Delta r_i$.

Calculation of the outer wall temperature

The inner wall temperature distribution was obtained from the finite difference solution. The outer wall temperature was com-

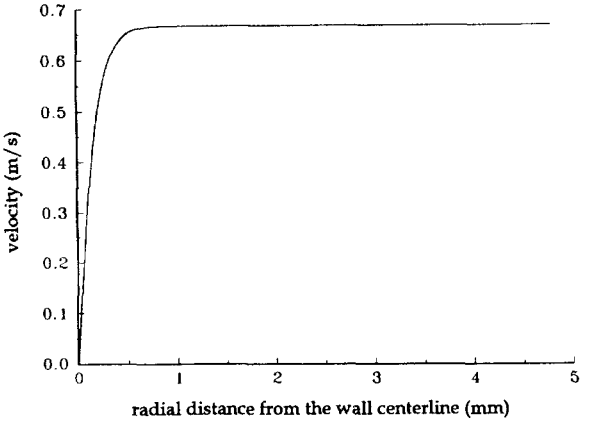

Figure 1 Velocity profile in the tube

puted by the assumption of steady state with heat flowing in the radial direction across the wall thickness. With the assumption that the rate of total heat transfer (power) was distributed uniformly on the heated surface of the tube, the inner wall heat flux q''_w was computed based on the inner surface area of the tube. This followed from the constant rate of heat transfer in the radial direction. Steady-state formulation yielded (Holman 1990)

$$T_0(x) = T_w(x) + \frac{q''_w R}{k} \ln\left(\frac{D_0}{D}\right) \tag{13}$$

where R denotes the inner radius of the tube.

Results and discussion

The numerical solution for each run considered yielded a mean velocity that was not more than 1.44% different from the corresponding experimental value. This difference took into account both the reliability factor in the linear regression analysis in determining C_L and C_T (which were fixed for each tube) as well as the numerical errors in computing the mean velocity of the flow. The velocity profile for a sample case with Re = 6300 for Tube #1 is shown in Figure 1. The good agreement between the numerical and experimental values of the mean (superficial) velocity of the flow also yielded very good agreement between the numerical and experimental values of the friction factor computed by using Equation 9. This comparison is depicted in Figure 2 for the runs with Tubes #1 and #2.

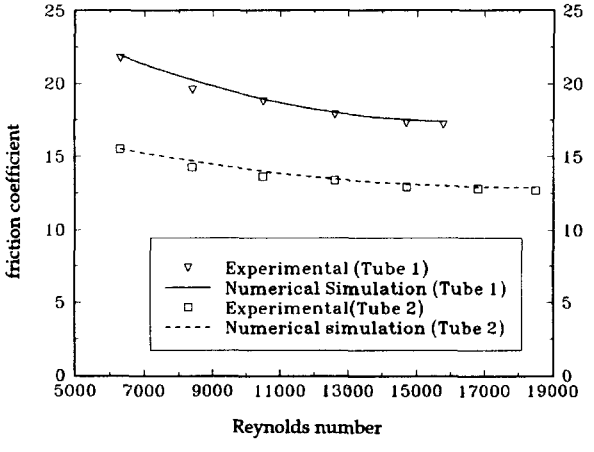

Figure 2 Variation of friction factor with Reynolds number

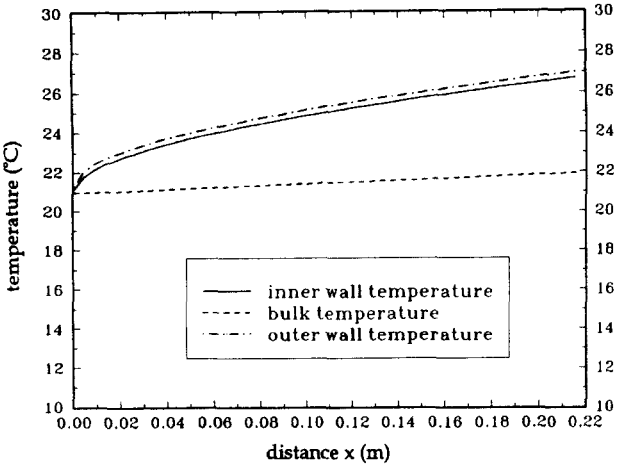

Figure 3 Various temperature distributions along the tube

The variation of different temperatures along the length of the tube for a typical run are depicted in Figure 3. The only temperatures measured in the experiments were those of the outer wall at specific locations and the mixed mean inlet and outlet temperatures. The measured outer wall temperatures and the corresponding simulated values for one run for each tube are shown in Figure 4. In general, the numerical simulation predicts slightly higher wall temperatures.

The variation of the local heat transfer coefficient along the tube wall was determined after the variation of the mean (bulk) temperature was obtained from the numerical simulations. The variation of the local heat transfer coefficient computed for a typical case with Re = 6300 for Tube #1 by using three different finite difference nodal meshes; namely, 51×51, 51×81, and 71×51 nodes is depicted in Figure 5. It can be seen from this figure that 51×51 nodes provide sufficiently accurate results.

Finally, the average heat transfer coefficient and the average Nusselt number for the total tube length were computed for each run for each tube. This was performed by taking the arithmetic mean of the local heat transfer coefficient (or Nusselt number) values at all the nodes on the inner wall of the tube with the exception of the first node, which is a singular point. These average values were compared with those determined experimentally in which the assumptions that were made included linear bulk temperature variation and an average heat transfer coeffi-

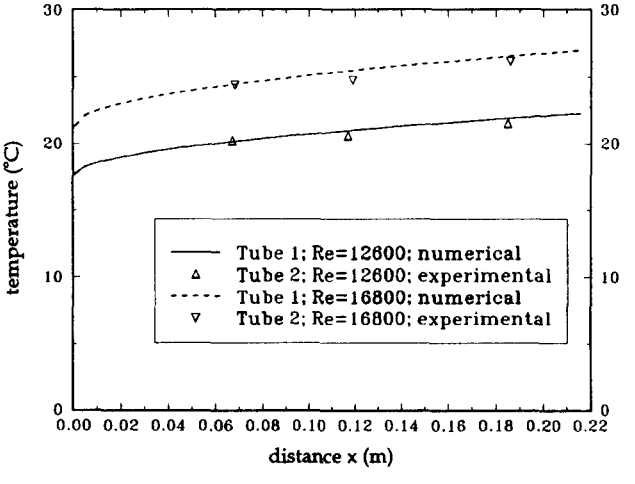

Figure 4 Variation of the outer wall temperature along the tube

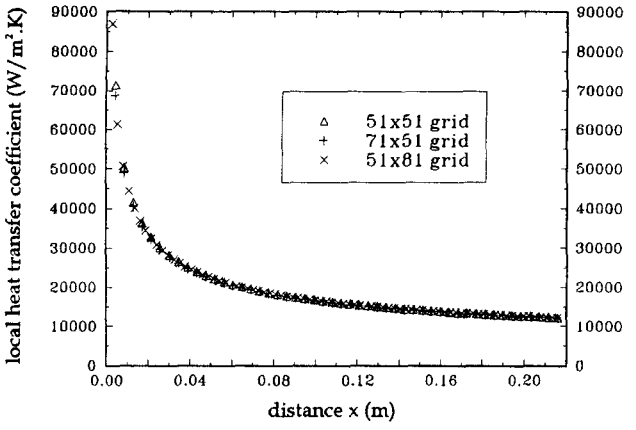

Figure 5 Variation of local heat transfer coefficient along the tube

cient that was evaluated at the midpoint of the tube (Kuzay et al. 1991). The comparison between the numerical results and the experimental ones is depicted in Figures 6 and 7. The general trend in these numerical simulations is slight under prediction of the heat transfer coefficient (or Nusselt number) at larger Reynolds numbers. Although this may not be seen in the case of Tube #1 for the lower Reynolds number range, the discrepancy was in the experimental data for which the steady state was not obtained properly. The primary reason for the underprediction of the heat transfer coefficient and the overprediction of outer wall temperature is that we used a conservative value for the effective thermal conductivity for the porous matrix. The constant n in Equation 5 was reported (Koh and Fortini 1971) to vary between 8 and 12 for porous copper. Moreover the experiments reported in the same reference were conducted with air rather than water as the fluid medium. Therefore, the value of 10 used in our simulations should be considered a conservative estimate. The numerical simulations were actually repeated by setting n to be equal to 8. With this adjustment, although the outer wall temperatures predicted from numerical simulations slightly improved, the heat transfer coefficient was overpredicted. Hence, we reported the more conservative results. Note that, in numerical simulation of this type of problem, one of the most challenging aspects is the selection of the model to be used for the effective thermal conductivity of the porous matrix, because there is usually very limited information relevant to the specific problem under investigation. Moreover, most theoretical models overpredict the effective thermal conductivity. Researchers should, therefore, exercise caution in choosing a theoretical or empirical model.

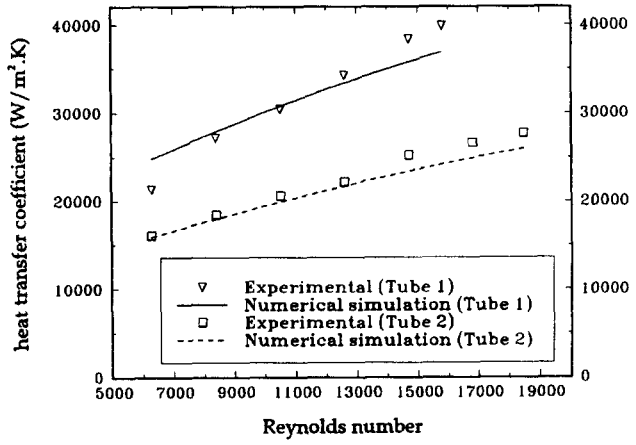

Figure 6 Variation of average heat transfer coefficient with Reynolds number

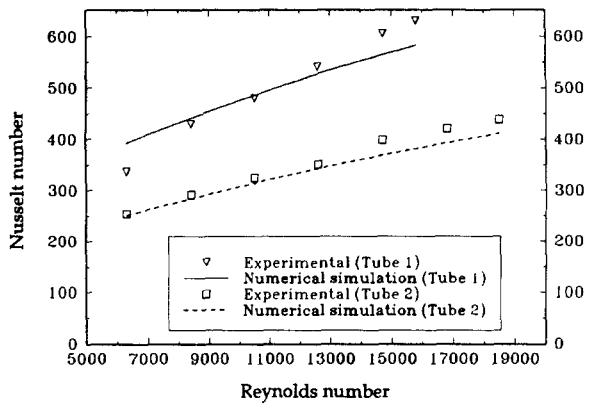

Figure 7 Variation of average Nusselt number with Reynolds number

It should be emphasized that the enhancement in heat transfer by the use of porous inserts will be at the cost of a large pressure drop. A pressure drop of such magnitude may not be allowable in certain applications. A method to improve this aspect would be the use of more structured porous inserts that will result in less form drag in the longitudinal direction. One example that could be suggested is a brush-type porous insert consisting of pins fixed on an axial rod at regular angles. However, it should also be ensured that as the pressure drop is improved, the effective thermal conductivity of the porous structure will not decrease considerably.

Acknowledgment

This work was supported by the U.S. Department of Energy, BES-Materials Sciences, under contract No. W-31-109-ENG-38.

References

Anderson, D. A., Tannehill, J. C. and Pletcher, R. H. 1984. *Computational Fluid Mechanics and Heat Transfer*. Hemisphere, Bristol, PA

Brinkman, H. C. 1947. A calculation of the viscous force exerted by a flowing fluid on a dense swarm of particles. *App. Sci. Res.*, **1**, 27–34

Cai, Z. 1993. Evaluation of the non-Darcy flow through fibrous media. *J. Mat. Proc. Manu. Sci.*, **2**, 19–39

Ergun, S. 1952. Fluid flow through packed columns. *Chem. Eng. Progress*, **48**, 89–94

Gortyshov, Y. F., Nadyrov, I. N., Ashikmin, S. R. and Kunevich, A. P. 1991. Heat transfer in the flow of a single-phase and boiling coolant in a channel with a porous insert. J. Eng. *Phys. Thermophysics*, **60**, 292–296

Holman, J. P. 1990. *Heat Transfer*, 7th ed., McGraw-Hill, New York

Januzewski, J., Khokhar, M. I. and Mujumdar, A. S. 1977. Thermal conductivity of some porous metals. *Lett. Heat Mass Transfer*, **4**, 417–423

Koh, J. C. Y. and Fortini, A. 1971. Thermal conductivity and electrical resistivity of porous material. Topical Report, NASA CR-120854

Kuzay, T. M. 1990. Fixed mask assembly research for the APS insertion device. ANL-90/20

Kuzay, T. M. 1994. A review of thermo-mechanical considerations of high temperature materials for synchrotron applications. *Nuclear Inst. Methods Phys. Res., A*, **347**, 644–650

Kuzay, T. M., Collins, J. T., Khounsary, A. M. and Morales, G. 1991. Enhanced heat transfer with metal wool-filled tubes. *Proc. of ASME / JSME Thermal Engineering Conference*, 145–151

Megerlin, F. E., Murphy, R. W. and Bergles, A. E. 1974. Augmentation of heat transfer in tubes by use of mesh and brush inserts. *J. Heat Transfer*, 145–151

Nakamura, S. 1986. Lecture notes for ME/NE 707, Winter 1986, The Ohio State University, Columbus, OH

Poulikakos, D. and Renken, K. 1987. Forced convection in a channel filled with porous medium, including effects of flow inertia, variable porosity and Brinkman friction. *J. Heat Transfer*, **109**, 880–888

Rosenfeld, J. H. and Lindemuth, J. E. 1993. Evaluation of porous media heat exchangers for plasma facing components *Proc. 15th IEEE / NPSS Symposium on Fusion Engineering*

Vafai, K. and Sözen, M. 1990. Analysis of energy and momentum transport for a fluid flow through a porous bed. *J. Heat Transfer*, **112**, 690–699